Journal of Medicinal Chemistry

Article

pubs.acs.org/jmc

Discovery of Diarylhydantoins as New Selective Androgen Receptor Modulators

François Nique,[†] Séverine Hebbe,[†] Christophe Peixoto,[†] Denis Annoot,[†] Jean-Michel Lefrançois,[†] Eric Duval,[†,§] Laurence Michoux,[†,∥] Nicolas Triballeau,[†] Jean-Michel Lemoullec,[†,⊥] Patrick Mollat,[†] Maxime Thauvin,[‡] Thierry Prangé,[‡] Dominique Minet,[†] Philippe Clément-Lacroix,[†] Catherine Robin-Jagerschmidt,[†] Damien Fleury,[†] Denis Guédin,[†,⊥] and Pierre Deprez*[,†]

[†]GALAPAGOS, Parc Biocitech, 102 Avenue Gaston Roussel, 93230 Romainville, France

[‡]UMR 8015 CNRS, Université Paris Descartes, 4 Avenue de l'Observatoire, 75006 Paris, France

Supporting Information

ABSTRACT: A novel selective androgen receptor modulator scaffold has been discovered through structural modifications of hydantoin antiandrogens. Several 4-(4-hydroxyphenyl)-*N*-arylhydantoins displayed partial agonism with nanomolar in vitro potency in transactivation experiments using androgen receptor (AR) transfected cells. In a standard castrated male rat model, several compounds showed good anabolic activity on levator ani muscle, dissociated from the androgenic activity on ventral prostate, after oral dosing at 30 mg/kg. (+)-4-[3,4-Dimethyl-2,5-dioxo-4-(4-hydroxyphenyl)imidazolidin-1-yl]-2-(trifluoromethyl)benzonitrile ((+)-**11b**) displayed anabolic potency with a strong dissociation between levator ani muscle and ventral prostate (A_{50} = 0.5 mg/kg vs 70 mg/kg). The binding modes of two compounds, including (+)-**11b**, within the AR ligand-binding domain have been studied by cocrystallization experiments using a coactivator-like peptide. Both compounds bound to the same site, and the overall structures of the AR were very similar.

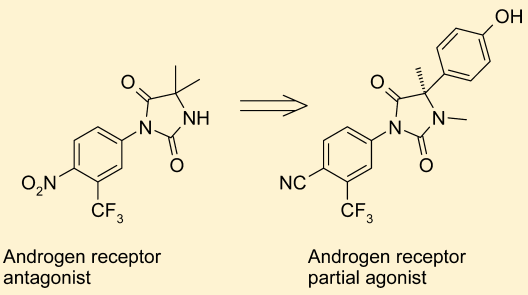

INTRODUCTION

In males, testosterone (T) and 5α-dihydrotestosterone (DHT) are the endogenous hormones which drive sexual development at puberty, maintenance of bone and muscle mass and strength, body composition, and sexual function in adulthood. The physiological effects of androgens are mediated by the androgen receptor (AR), which belongs to the nuclear hormone receptor superfamily of intracellular ligand-dependent transcription factors. Deficiencies in circulating androgen levels in male serum can be caused either by hypogonadism or more often by the aging process, which leads to musculoskeletal functional decline and other effects.[1] Cognitive disorders such as Alzheimer's disease have also been linked to testosterone deficiency.[2] It has been shown clinically that administration of testosterone at physiological doses in elderly men improves both muscle strength and body composition.[3] However, unlike estrogen replacement therapy, which has found extensive use in menopausal women, androgen replacement therapy is not widely used due to potential side effects. The main concern about testosterone replacement therapy is the possible impact on the prostate, i.e., increase in benign prostatic hypertrophy and/or stimulation of a nondiagnosed prostate cancer.[4] Moreover, because of its steroidal structure, testosterone is not orally available due to rapid first pass metabolism in the liver which produces DHT and estrogens.

Many efforts were initiated a decade ago to find orally available nonsteroidal androgens.[5] The improvements in safety that were achieved in nonsteroidal selective estrogen receptor modulators (SERMs) in postmenopausal women[6] prompted the search for selective androgen receptor modulators (SARMs) for male use.[7] These compounds should offer a better distinction between desired anabolic and unwanted androgenic properties. Turning nonsteroidal androgen receptor antagonists into orally active agonists has already been accomplished with several chemical scaffolds as exemplified by the bicalutamide-derived propionamides **1** (andarine)[8] and **2** (ostarine)[9] or the design of the fused bicyclic hydantoin **3** (BMS-564929)[10] shown in Figure 1. Compounds from both series have been developed, and some have reached the clinical stage.[11]

Our own early discovery program led us to investigate the *N*-arylhydantoin core of the antiandrogen nilutamide (**4**)[12] as a starting point. We have identified (*R*)-(+)-4-[3,4-dimethyl-2,5-dioxo-4-(4-hydroxyphenyl)imidazolidin-1-yl]-2-(trifluoromethyl)benzonitrile [(*R*)-(+)-**11b**] as a new SARM from structure−activity relationship (SAR) studies in a series of 1-aryl-4-(4-hydroxyphenyl)hydantoins. Compound (+)-**11b** displayed tissue selectivity in animal models upon oral

Received: February 23, 2012
Published: August 16, 2012

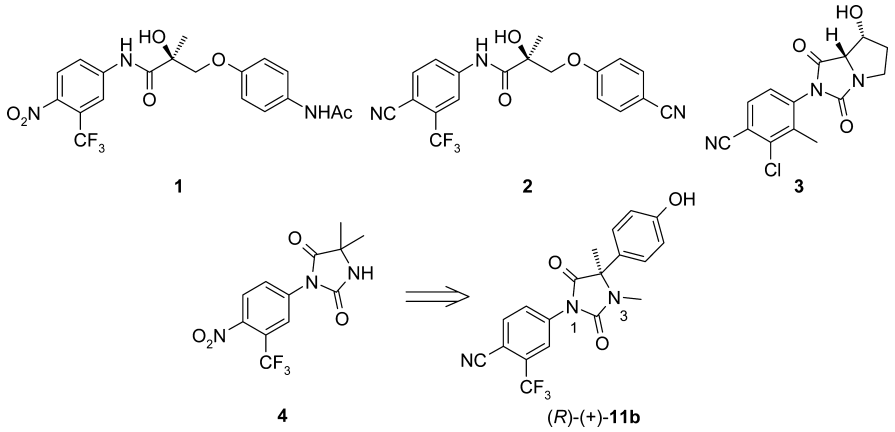

Figure 1. Nonsteroidal androgen receptor ligands.

Scheme 1[a]

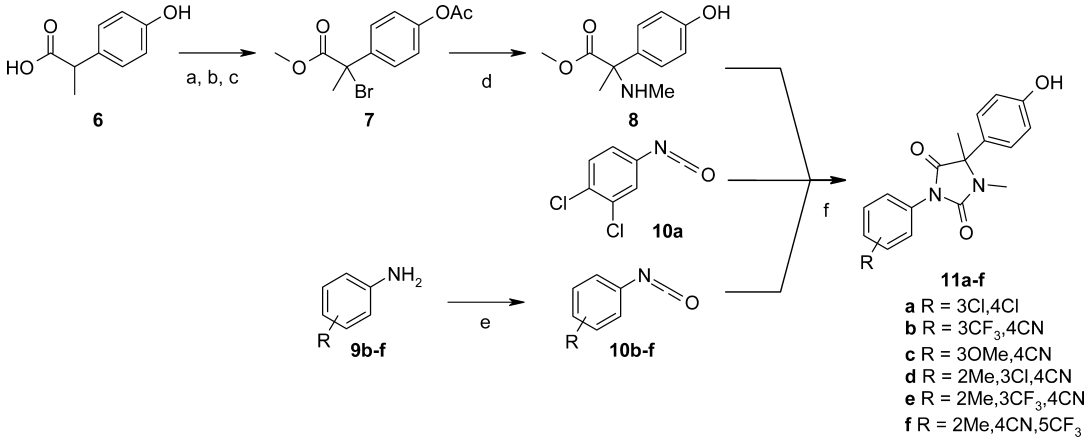

[a]Reagents and conditions: (a) $SOCl_2$, MeOH, 0 °C; (b) Ac_2O, K_2CO_3, THF; (c) NBS, AIBN, CCl_4, reflux, 100% (three steps); (d) $MeNH_2$, EtOH, 78%; (e) triphosgene, toluene/dioxane, 110 °C, (96−100%); (f) THF, reflux, 45−96%.

administration with a reduced androgenic effect on prostate compared to anabolic activity on muscle. Structural analyses from this new series have been used to obtain insight into the features driving tissue selectivity. Herein we report the discovery of this new biarylhydantoin SARM scaffold.

CHEMISTRY

The general synthesis of hydantoins (±)-**11a−f** is depicted in Scheme 1. These compounds were prepared by condensation of amino ester **8** and commercially available isocyanate **10a** or isocyanates **10b−f**, obtained from the corresponding anilines **9b−f** (96−100%). The amino ester **8** was obtained from 2-(hydroxyphenyl)propionic acid (**6**) through successive esterification, acetylation, and bromination α to the aryl ring to provide the bromo ester **7** (quantitative overall yield). Treatment of **7** with an ethanolic solution of methylamine gave rise to the amino ester **8** (78%) through substitution of the bromo atom and in situ deprotection of the acetate group. The ring-forming condensation of **8** on the isocyanates **10a−f** provided the diarylhydantoins **11a−f** as racemic mixtures (45−96%).

The racemate (±)-**11b** was resolved by chiral HPLC to provide the single enantiomers (+)-**11b** and (−)-**11b**. Assignment of the absolute stereochemistry (*R* and *S*, respectively) was done by comparison of these enantiomers with the authentic compounds prepared by enantioselective synthesis as described below.

Analogous thiohydantoins (±)-**13a,b** were prepared in a similar manner by coupling the amino ester **8** with the appropriate thioisocyanates **12a,b**. Thioisocyanate **12a** is commercially available, and **12b** was prepared by reacting aniline **9b** and thiophosgene (Scheme 2).

Substitution of the bromo atom of **7**, by either allylamine or propargylamine, provided the amino esters **14** and **16**, respectively (Scheme 3). Coupling of isocyanate **10b** and **14**

Scheme 2[a]

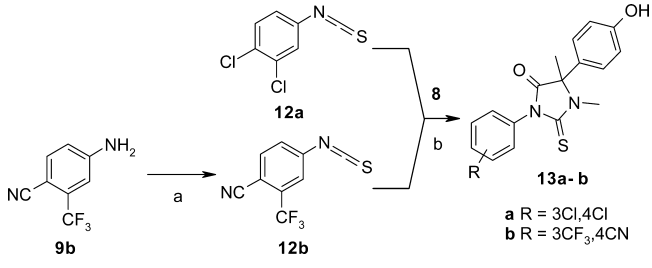

[a]Reagents and conditions: (a) $CSCl_2$, H_2O, rt, 86%; (b) NEt_3, THF, rt, 18 h, 75−77%.

dx.doi.org/10.1021/jm300249m | J. Med. Chem. 2012, 55, 8225−8235

or **16** produced the hydantoins (±)-**15b** (73%) and (±)-**17b** (89%).

Scheme 3[a]

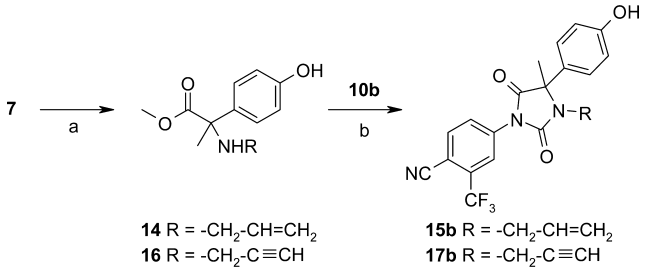

[a]Reagents and conditions: (a) allylamine or propargylamine, THF, rt, 30 min; (b) THF, reflux, 73–89%.

The individual enantiomers (−)-**11b**, (+)-**11b**, and (+)-**11c** have been prepared enantiopure according to an analogous route, coupling the appropriate isocyanates with the suitable enantiomerically pure amino ester. As the synthesis of the chiral *N*-methylamino esters (*S*)-**8** and (*R*)-**8** was not obvious, we used methyl 2-amino-2-(4-methoxyphenyl)propionates (*S*)-(+)-**20** and (*R*)-(−)-**20** as the starting materials (Scheme 4). The synthesis of the ethyl ester homologue of (*S*)-(+)-**20** has been described in the literature.[13] We used a similar process to prepare (*S*)-(+)-**20** by simply replacing ethanol with methanol in the final esterification step. (*R*)-(−)-**20** was obtained by the same sequence using (*R*)-(+)-α-methylbenzylamine as the resolving base instead of its (*S*)-(−)-enantiomer.

The amino ester (*R*)-(−)-**20** was coupled to the isocyanates **10b** and **10c** to produce hydantoins (*R*)-(+)-**21b** and (*R*)-(+)-**21c** in excellent yields (95–97%). These compounds were further subjected to an N-methylation, O-demethylation sequence to provide the hydantoins (*R*)-(+)-**11b** (77%) and *R*-(+)-**11c** (54%). The enantiomer (*S*)-(−)-**11b** was prepared the same way using the amino ester (*S*)-(+)-**20**.

It was not possible to prepare *N*-alkylthiohydantoins using this method due to the higher reactivity of the thiocarbonyl vs the intracyclic nitrogen toward alkylation. To prepare the N-methylated thiohydantoin (*R*)-(+)-**13a**, the amino ester (*R*)-(−)-**20** was converted to its *o*-nitrophenyl sulfonyl derivative **22** (40%) to allow an easy N-alkylation (Scheme 5). Methylation of **22** followed by sulfonamide cleavage proceeded in good yield (85%). The amino ester *R*-(−)-**23** thus obtained was then subjected to coupling with thioisocyanate **12a** (95%) and then O-demethylation to yield the thiohydantoin *R*-(+)-**13a** (70%).

As described below, the *R* absolute configurations of compounds (+)-**11b** and (+)-**13a** have been further confirmed by solving the cocrystal structure of each compound bound to the ligand-binding domain of the androgen receptor (AR LBD).

RESULTS AND DISCUSSION

To identify an SARM, we needed to choose compounds that display a strong dissociation between the prostate (where ideally the compound should not be an agonist) and muscle and/or bone (where ideally it should be a stronger agonist). Since the same androgen receptor is expressed in all three tissues, the origin of an SARM profile is not likely to be traced back by a strong differential tissue potency. Conversely, partial activation of the AR might lead to the desired tissue selectivity. The reason for this prospect is explainable within the framework of the Monod–Wyman–Changeux model,[14] where the receptor is in equilibrium between two states, the resting state (R) and the active state (A). We believe this model provides a perfect framework for evaluation of partial agonism. Any ligand of the receptor actually has two molecular affinities for the receptor: one for the active state A (denoted K_A) and one for the inactive state R (denoted K_R). Applying the law of mass action to each of the two states leads to the potency equation.

In the absence of ligand, the equilibrium constant *L* is the ratio between the resting and active states of the receptor, and this equilibrium is tissue dependent. In a given tissue, a ligand will shift the equilibrium constant *L* by a factor depending on the ratio of its two affinities for the two states K_R and K_A. We

Scheme 4. Synthesis of Pure Enantiomers (*R*)-(+)-11b–c[a]

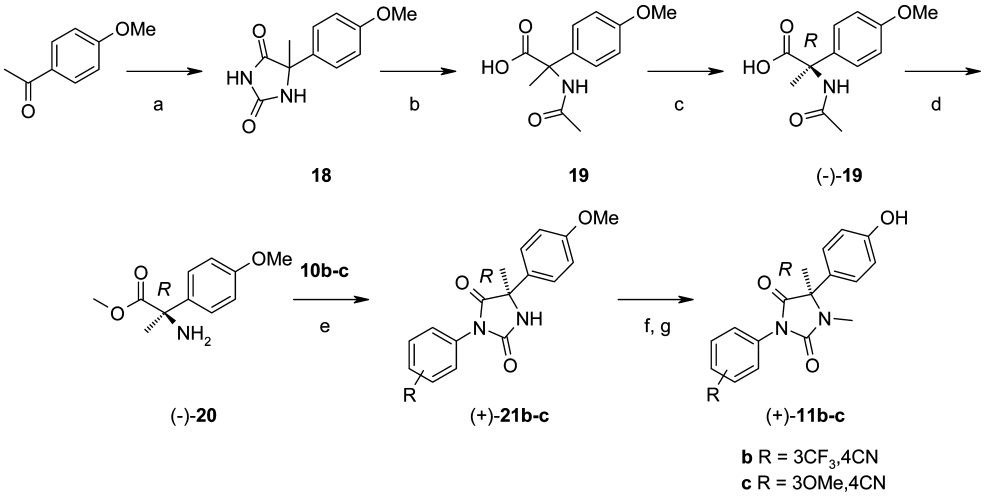

[a]Reagents and conditions: (a) $(NH_4)_2CO_3 \cdot H_2O$, KCN, EtOH, H_2O, 55 °C, 3 h, 99%; (b) NaOH, Ac_2O, reflux, 64 h, 93%; (c) (*R*)-(+)-α-methylbenzylamine, EtOH, 40 °C, then HCl (2 N), 31%; (d) HCl (4 N), reflux, 4 h, then HCl, MeOH, reflux, 15 h, then $NaHCO_3$, 84% (two steps); (e) THF, NEt_3, reflux, 2 h, 95–97%; (f) NaH, MeI, DMF, rt, 20 min; (g) $BF_3 \cdot Me_2S$, rt, 54–77% (two steps).

dx.doi.org/10.1021/jm300249m | J. Med. Chem. 2012, 55, 8225–8235

Scheme 5. Synthesis of Pure Enantiomer (*R*)-(+)-13a[a]

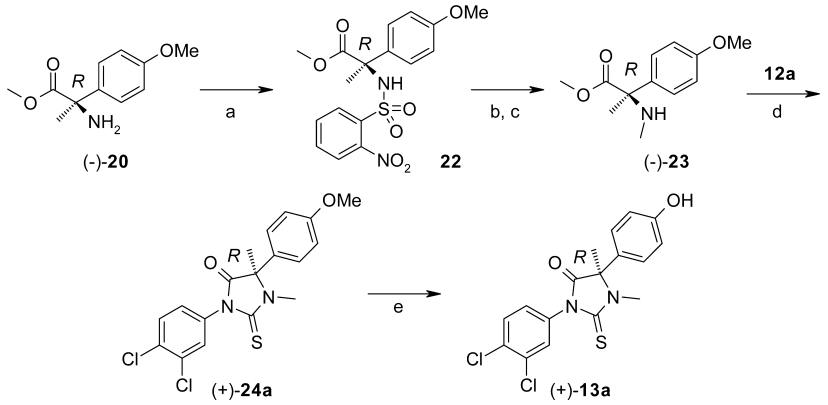

[a]Reagents and conditions: (a) 2-NO_2PhSO_2Cl, pyridine, 1.5 h, reflux, 40%; (b) NaH, MeI, DMAC, 3 h, rt; (c) K_2CO_3, thiophenol, DMAC, 2 h, rt, 85% (two steps); (d) THF, NEt_3, rt, 1 h, 95%; (e) $BF_3{\cdot}Me_2S$, rt, 24 h, 70%.

Table 1. In Vitro and in Vivo Activities of 1-Aryl-4-(4-hydroxyphenyl)hydantoins

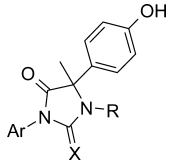

compd[a]	Ar	X	R	chiral center	in vitro potency (nM)	in vitro molecular efficacy	anabolic in vivo activity, levator ani muscle (%)	androgenic in vivo activity, ventral prostate (%)
TP[b]					1.5	600	99	73
(±)-**11a**	3-Cl-4-ClPh	O	Me	*RS*	10.9	150	12	0
(±)-**11b**	3-CF_3-4-CNPh	O	Me	*RS*	1.6	114	84	14
(−)-**11b**	3-CF_3-4-CNPh	O	Me	*S*	200	48	−5	5
(+)-**11b**	3-CF_3-4-CNPh	O	Me	*R*	0.9	132	75	25
(±)-**11c**	3-OMe-4-CNPh	O	Me	*RS*	2.1	141	96	51
(+)-**11c**	3-OMe-4-CNPh	O	Me	*R*	1.5	200	132	30
(±)-**11d**	2-Me,3-Cl-4-CNPh	O	Me	*RS*	1.5	300	82	12
(±)-**11e**	2-Me-3-CF_3-4-CNPh	O	Me	*RS*	3	100	nd	nd
(±)-**11f**	2-Me-4-CN-5-CF_3Ph	O	Me	*RS*	200	10	nd	nd
(±)-**13a**	3-Cl-4-ClPh	S	Me	*RS*	2	122	13	0
(+)-**13a**	3-Cl-4-ClPh	S	Me	*R*	0.8	200	nd	nd
(±)-**13b**	3-CF_3-4-CNPh	S	Me	*RS*	4	80	12	4
(±)-**15b**	3-CF_3-4-CNPh	O	allyl	*RS*	2	89	15	−3
(±)-**17b**	3-CF_3-4-CNPh	O	propargyl	*RS*	2.4	110	95	19

[a]All the test compounds except (+)-**11c** were administered orally with a dose of 30 mg/kg; (+)-**11c** was administered orally with a dose of 10 mg/kg. [b]Testosterone propionate (TP) was administered subcutaneously at 1 mg/kg.

call this ratio K_R/K_A the molecular efficacy since it directly reflects the amplitude of the discrimination the ligand exerts between the two states of the androgen receptor. To bring the activation in a range where it will have an effect, the discrimination (i.e., molecular efficacy of the ligand) must overwhelm the tissue-dependent initial position L of the equilibrium: a smaller L will allow a compound with a smaller efficacy to be active, whereas a larger L will require a stronger molecular efficacy. In other words, if two tissues differ by a factor of 10 in their L constants (ratio between the resting and active states of the receptor), the tissue with the smallest L will allow a partial agonist to display activity whereas the tissue with a 10-fold larger L will see it as a neutral antagonist. A highly discriminated compound (i.e., high molecular efficacy, also meaning full agonist) will show agonist activity anyway in the two tissues. Therefore, the success of the approach using the

dx.doi.org/10.1021/jm300249m | J. Med. Chem. 2012, 55, 8225−8235

Monod−Wyman−Changeux model lies in the hope that tissues may differ in their initial position of the equilibrium between the resting and the active states, with prostate having an equilibrium shifted more toward the inactive state than bone and muscle, thus allowing compounds with a moderate molecular efficacy to display their activity in one tissue (bone and muscle) and not in the other (prostate). This hypothesis, although not formally established, offers the great advantage to discriminate the parameters linked to the compound (i.e., the molecular efficacy K_R/K_A) and the parameter linked to the tissue (i.e., equilibrium constant L). Of course, the position of the equilibrium between the active and inactive states of the androgen receptor in the different tissues is not the only explanation of the tissue selectivity. Densities of androgen receptor and spare receptors and concentrations of coactivator and corepressor also vary from one tissue to the other, and all these factors play a role in the overall tissue selectivity. In our approach, we focused essentially on the identification of partial agonists with limited activity even at saturation. For this purpose, we used the Monod−Wyman−Changeux model heuristically, combining in vitro data (partial agonism) and in vivo data (in vivo tissue selectivity) and actually found it convenient and reliable to progress along the exploration of the chemical series.

The scale we chose ascribes a molecular efficacy of 4000 to DHT (full agonist) and 1 to nilutamide (neutral antagonist). Viewed as a log scale, the middle of this window (between 30 and 300) appeared to us as defining the compounds having intermediate molecular efficacy, thus qualifying them for the nomination of partial agonists, potentially capable to display tissue selectivity. Then, on selected compounds, we confirmed in vivo that the in vitro partial agonism profile converts to tissue selectivity with limited activity on the prostate and higher activity on muscle or bone in the Hershberger model.

Practically, to evaluate in vitro potency and molecular efficacy of our compounds, we set up a transcriptional assay using the Hela cell line transfected with hAR receptor and with an androgen-responsive element (ARE) coupled with luciferase. For each SARM compound prepared, we generated dose−response curves, crossing a range of concentrations of DHT with a range of concentrations of our SARM compound. In this transcriptional assay, potency for DHT is 8 nM and molecular efficacy 4000. We observed modifications of the DHT dose−response curve when different concentrations of SARM were added. This led to the identification of SARM compounds with potency of 1−10 nM and efficacy of 30−150. When looking at the shape of the curves, the Hill coefficient of our SARM compounds in the in vitro transactivation assay appears to be close to 1, thus indicating no apparent cooperativity. This assay was also validated using a reference compound that progressed in clinical development, such as ostarine (**2**), known for its tissue-selective anabolic effect.[7c] In our assay, **2** had good potency (1.5 nM) and a molecular efficacy of 60, which in our assay indicates partial agonism.

4,4-Dimethylhydantoins[15] have long been known as antagonists to the androgen receptor, as exemplified by nilutamide (**4**).[12] Replacement of one methyl of this hydantoin core by a phenyl ring did not change the antagonistic nature of the molecule in vitro (potency 37 nM, molecular efficacy 3), nor did the corresponding 4-methoxyphenyl analogue (*N*-methyl analogue of **21b**, potency 150 nM, molecular efficacy 1). However, the introduction of a 4-hydroxyphenyl group as in compounds **11a−f** turned their profile to partial agonism (potency 1−10 nM, molecular efficacy 100−300).

In Vitro Activity. The in vitro functional activity of 1-aryl-4-(4-hydroxyphenyl)hydantoins has been assessed in cells expressing human androgen receptor (hAR). The results of transcriptional activities of compounds **11a−f**, **13a,b**, **15b**, and **17b** are listed in Table 1 as potency and molecular efficacy values.

Most of the compounds displayed a partial agonist profile. The N-substituents evaluated at position 3 of the hydantoin core did not influence the activity in the cell-based assay: *N*-methyl (±)-**11b**, *N*-allyl (±)-**15b**, and *N*-propargyl (±)-**17b** displayed similar potencies (potency 1.6, 2, and 2.4 nM, respectively), in the range of that of DHT. However, compared to that of DHT, the molecular efficacy was much lower for these three compounds (around 100 vs 4000), in agreement with our goal of identifying partial agonists. As a consequence, further optimization was carried out around similar compounds as described in Table 1, with the simplest methyl substituent on the nitrogen in position 3. Substituents of the *N*-phenyl in position 1 had a pronounced effect on potency, but for the most part maintained the profile of a partial agonist. One of the most potent compounds of the series, (±)-**11b**, contained a 4-cyano-3-(trifluoromethyl)phenyl, which is present in many AR ligands. Replacement of the electron-withdrawing trifluoromethyl group in (±)-**11b** by the electron-donating methoxy group led to (±)-**11c**, with a similar in vitro profile (potency 2.1 nM). On the other hand, compound (±)-**11a** bearing a 3,4-dichlorophenyl was 10 times less potent than (±)-**11b** (potency 10.9 nM) due to a lack of a H-bond acceptor group such as cyano. Several trisubstituted phenyl derivatives were explored with (±)-**11d** and (±)-**11e**, which retained potency similar to that of (±)-**11b**, indicating that some steric hindrance in position 2 of that phenyl ring was tolerated. On the other hand, the 4-cyano-2-methyl-5-(trifluoromethyl)phenyl (±)-**11f** was much less potent (potency 200 nM) than the isomeric (±)-**11e** and behaved more like an antagonist with a molecular efficacy of 10. In (±)-**11f** the steric hindrance was much more pronounced than in (±)-**11e** as two substituents are on opposite sides of the phenyl ring, precluding a correct fit in the binding pocket of the AR. The configuration at the chiral center had a strong effect on the activity in the cell-based assay. Compound (±)-**11b** has been resolved into its pure enantiomers, which were tested for AR transcriptional activity. Compound (+)-**11b** appeared to be >200-fold more potent (potency 0.9 nM) than its antipode (−)-**11b** (potency 200 nM) and 2-fold more potent than the racemate, as expected. Compound (+)-**11b** was also confirmed as a partial agonist with a molecular efficacy of 132, allowing a theoretical differentiation between prostate and muscle and bone tissue (confirmed in the in vivo experiments). After both *R* and *S* stereoselective syntheses had been performed (Scheme 4), the *R* configuration was attributed to the more potent (+)-**11b** and the *S* configuration to (−)-**11b**. This was confirmed by structural analysis of (+)-**11b** cocrystallized with hAR LBD. The *R* enantiomer of **11c** has been similarly prepared, giving rise to (+)-**11c**, which showed an almost 2-fold higher activity compared to the racemic mixture (±)-**11c** (potency 1.5 and 2.1 nM, respectively). In competitive binding assays (+)-**11b** was specific for AR with an IC_{50} of 9.6 nM. A weak binding was recorded for the progesterone receptor (IC_{50} = 8.8 μM) with no significant binding of the estrogen and glucocorticoid receptors up to 10 μM.

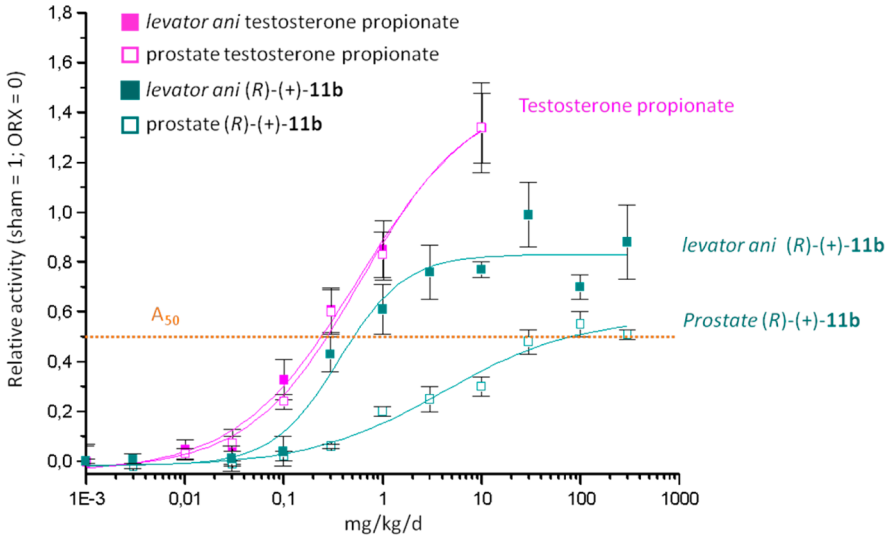

Figure 2. Comparison of the anabolic versus androgenic activities of (+)-**11b** and testosterone propionate in ORX rats. A_{50} = dose displaying 50% activity on levator ani or ventral prostate.

Replacement of the urea carbonyl of the hydantoin ring by a thiocarbonyl gave rise to the thiohydantoins (±)-**13a** and (±)-**13b**. These two compounds are potent and partial agonists (molecular efficacy 122 and 80), but the detailed effect of this replacement is compound dependent. A 5-fold increase in transcriptional activity was recorded with thiohydantoin (±)-**13a** (potency 2 nM) compared to the hydantoin (±)-**11a**, while a 2-fold decrease was noticed with thiohydantoin (±)-**13b** (potency 4 nM) versus the hydantoin (±)-**11b**. Nevertheless, the *R* enantiomer (+)-**13a** prepared stereospecifically was shown to be twice as active as the racemate (±)-**13a** (potency 0.8 nM) and partial agonist.

In Vivo Activity. As several of these compounds displayed activity profiles of partial agonists in vitro with potencies close to that of testosterone, we evaluated the ability of these compounds to be tissue selective by stimulating muscle anabolism with limited effect on prostate growth in an orchidectomized (ORX) rat model. In this model, young castrated rats are left untreated for one week and then treated orally for four successive days with a partial agonist at 30 mg/kg. Untreated ORX rats and sham-operated animals were used as controls. Another control group was treated subcutaneously with 1 mg/kg testosterone propionate (TP). The weight of the levator ani muscle (LA) was considered a marker of anabolic activity, whereas the weight of the ventral prostate (VP) was regarded as a marker of androgenic activity.[16] Results of these experiments are shown in Table 1. At 30 mg/kg, partial agonists (±)-**11b**, (±)-**11c**, (±)-**11d**, and (±)-**17b** restored the weight of LA around that of sham control animals while the prostate weights remained far below those of intact animals, in accordance with their in vitro activities. This illustrates a significant distinction between the anabolic (muscle) and androgenic (prostate) effects and correlation with the in vitro profiling of the compounds. The pure enantiomers (+)-**11b** and (+)-**11c** behaved similarly, and the antipode molecule (−)-**11b** was inactive, as expected from its lower in vitro activity. Another less potent compound, the dichlorophenyl (±)-**11a**, did not show any activity either. Despite good profiles, *N*-allyl derivative (±)-**15b** and the thiohydantoin (±)-**13b** were devoid of any in vivo activity. The reasons were not investigated and could be due to lack of oral bioavailability and/or a higher susceptibility to metabolism caused by the presence of the sulfur atom (for the thiohydantoins). On the other hand, the *N*-propargyl (±)-**17b** and *N*-methyl (±)-**11b** with very similar in vitro profiles (potencies and molecular efficacies) also behaved in the same way in vivo with a potent anabolic activity on muscle and strong tissue differentiation versus prostate (95−84% on LA muscle compared to 19−14% effect on VP). **11b** was preferred to **17b** for further studies due to a potential toxicity of the triple bond in **17b** (linked to possible oxidation of the triple bond and formation of further reactive metabolites).

To further explore the anabolic potency and tissue selectivity of (+)-**11b**, a wide dose-range experiment was performed in comparison with TP. TP showed similar dose−response curves for both LA and VP with A_{50} = 0.30 and 0.20 mg/kg, respectively, A_{50} being the active dose that induced 50% activity (sham, 1; ORX, 0) (Figure 2) and a maximal effect on both LA and VP of 130% (vs sham). Conversely, (+)-**11b** demonstrated an A_{50} similar to that of TP on LA (A_{50} = 0.50 mg/kg) with a maximal effect on LA around 80%. As expected, (+)-**11b** had a weak effect on VP (A_{50} = 70 mg/kg), showing a strong dissociation between anabolic and androgenic effects (factor of 140). Unlike TP, (+)-**11b** did not show an increase in LA weight over that of sham animals even at very high doses (300 mg/kg). In contrast to TP at this high dose, (+)-**11b** caused only a 50% increase of the VP weight, reflecting the partial agonist profile of (+)-**11b**. These data clearly demonstrate the tissue selectivity of (+)-**11b** and warrant its classification as an SARM.

The effect of compound (+)-**11b** on bone was also evaluated in an ORX rat model. In this model, six month old male rats were castrated and treated with 30 mg/kg (+)-**11b**, once daily, oral administration for three months in a preventive manner. As expected, the ORX surgery induced a significant bone loss as indicated by a BMD (bone mineral density, peripheral quantitative computed tomography (pQCT), Stratec) of −27% and a trabecular BV/TV (bone volume; μCT, Scanco) of −42% vs sham. The bone loss observed in ORX animals was fully prevented by (+)-**11b** on both BMD and BV/TV parameters. This protection was correlated with bone biomechanic properties of trabecular and cortical bones.

dx.doi.org/10.1021/jm300249m | *J. Med. Chem.* 2012, 55, 8225−8235

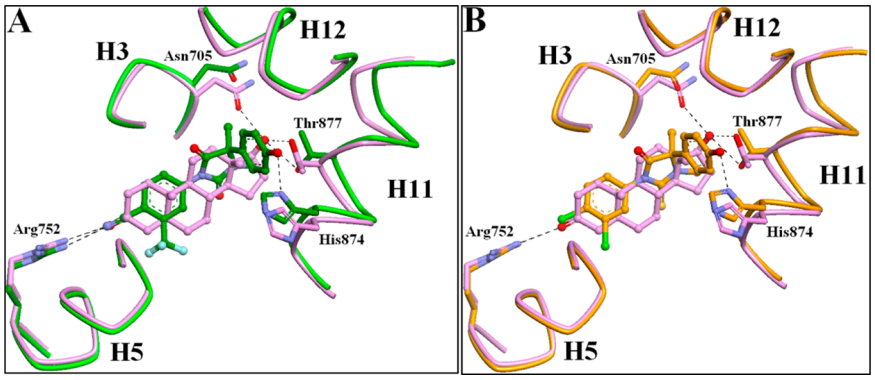

Figure 3. Superimposition of cocrystals of (+)-**11b** (A) and (+)-**13a** (B) with DHT. Each complex was superimposed on the cocrystal structure with DHT (PDB code 2AMA) in Discovery Studio[22] by minimizing the rmsd of the Cα traces. (A) Superimposition of (+)-**11b** with DHT. The complex of hAR LBD with (+)-**11b** is represented in green, and DHT is pink. The cyano group of (+)-**11b** maintains the same hydrogen bond with Arg752 that is observed in the complex with DHT. Conversely, at the opposite side of the compound, there is no equivalent of the hydrogen bond of DHT with Asn705 and Thr877. The hydroxyphenyl moiety of (+)-**11b** occupies a pocket almost perpendicular to DHT's hydroxyl group, which is involved in a direct hydrogen bond with His874. (B) Superposition of (+)-**13a** with DHT. The complex of hAR LBD with (+)-**13a** is represented in orange, and DHT is pink. As in the complex with (+)-**11b**, the hydroxyphenyl moiety occupies a pocket almost perpendicular to the DHT plane, and its hydroxyl group is involved in a direct hydrogen bond with His874.

Detailed bone data will be reported elsewhere. This indicates that the partial agonist (+)-**11b** is also effective in preventing ORX-induced bone loss, indicating that (+)-**11b** is active on bone in addition to muscle. Activities on prostate and LA after three months of treatment were 30% and 124%, respectively, after oral administration of (+)-**11b**, 30 mg/kg/day. Total cholesterol was significantly decreased by 2-fold in ORX rats treated with (+)-**11b** (the measure of HDL is not relevant in rats). Triglycerides were significantly decreased by 30% in ORX rats treated with (+)-**11b**.

Structural Biology and Crystallography. In an attempt to compare binding modes of DHT and our hydantoin compounds, cocrystals of the hAR LBD linked to a coactivator-like peptide[17] were obtained with (+)-**11b** and (+)-**13a**.[18] It has been shown that the binding of different ligands (agonist, antagonist) critically affects the position of helix H12, with respect to the interaction with different coregulators.[19] Both crystals generated in our work showed the agonist conformation of the AR LBD, with helix H12 in the position observed upon binding of DHT.[18] We considered the possibility that the presence of a coactivator peptide in the crystals might affect the dynamic of helix H12, but actually, in the absence of a coactivator peptide, the AR LBD adopted the same agonist conformation in the crystal structure with the partial agonist **1**.[20] This tends to indicate that the coactivator peptide does not force the agonist conformation but participates in the stabilization of the complex.The structures of the two hydantoin complexes are very similar with a root-mean-square deviation (rmsd) of 0.39 Å calculated on all the atoms. The hydantoin molecules were positioned in exactly the same way in the binding pocket, the *R* configuration being thus confirmed at their asymmetric centers.

Figure 3 displays a comparison of (+)-**11b** and (+)-**13a** to DHT in the hAR LBD binding pocket. The cyano group of (+)-**11b** is in the same position as the 3-keto group of DHT, allowing hydrogen bonding with residue Arg752 of the receptor protein (2.89 Å), like that of DHT (Figure 3A). The dichlorophenyl compound (+)-**13a** lacks the cyano group (Figure 3B), but remains as active as the cyano derivative (+)-**11b**. In both compounds, the hydroxyphenyl group extends from the core of the molecule at the same place as the 18-methyl of DHT. Conversely to what has been described for DHT,[18,21] no interaction with Thr877 and Asn705 was possible for (+)-**11b** and (+)-**13a**, but a further hydrogen bond was evident with His874 (2.77 Å for (+)-**11b** and 2.75 Å for (+)-**13a**). This has already been observed with the propionamide SARM **1**, which was described to interact with His874, albeit through a water molecule.[20] In all three cases, the binding of the compound induced a widening of the pocket so that the receptor could accommodate the protruding aryl groups.

When comparing the peptide chain of hAR LBD cocrystallized with either (+)-**11b** or (+)-**13a** and DHT, few differences were found. In the least-squares superposition of the coordinates, the average rmsd is 0.73 Å for (+)-**11b** and 0.62 Å for (+)-**13a** for all the main-chain atoms. In both cases, we were not able to observe electron density for the loop of five residues (845−849), as previously described.[18] Compared to DHT, we also observed that helix H11 was slightly kinked from Thr877 to its end and the loop connecting helices H11 and H12 (residues 883−891) was disordered, with a poor density fit. Therefore, no marked change was evident in the protein following binding with a full agonist (DHT) or partial agonist [(+)-**11b**, (+)-**13a**], making it difficult to explain on the protein level the observed partial agonism profile resulting in the tissue selectivity of (+)-**11b**. Nonetheless, it is possible that small changes around the ligand may alter the cofactor interaction profile. Moreover, domains of the AR other than the LBD were not included in this analysis and could play a major role in the selectivity of the ligands.

■ CONCLUSION

In conclusion, a new series of hydroxyphenyl-substituted arylhydantoins has been synthesized and characterized in vitro as partial androgen agonists. Their partial agonism profile and high affinity for the AR translates in vivo to tissue-selective pharmacologic activity when orally administered in a castrated rat model. Particularly, (+)-**11b** maintained the levator ani muscle weight with potency similar to that of testosterone while showing only weak stimulation of the prostate. The strong distinction between anabolic and androgenic activity in vivo is typical of an SARM. Moreover, (+)-**11b** prevented degradation

dx.doi.org/10.1021/jm300249m | *J. Med. Chem.* 2012, 55, 8225−8235

of bone loss after ORX. The new scaffold described herein constitutes a significant advance in the search of efficient and highly tissue-selective nonsteroidal SARMs. Compound (+)-**11b** proved to be an excellent tool validating our approach toward in vivo tissue selectivity from our in vitro tools around the hydantoin series. Further optimization around the hydantoin scaffold, keeping an in vivo selective profile similar to that of compound (+)-**11b**, will be reported soon.

EXPERIMENTAL SECTION

Unless otherwise stated, all procedures were performed under a nitrogen atmosphere using anhydrous solvents purchased from commercial sources. Thin-layer chromatography was performed using precoated Merck silica gel 60 F254 plates, visualized under UV light or after staining by spraying a solution of 20% phosphomolybdic acid in ethanol and then heating. Preparative chromatography was conducted on Merck silica gel 60 (0.040−0.063 mm). All ^{1}H NMR spectra were recorded using a Bruker DPX (300 MHz) or Advance (400 MHz) spectrometer, in solution in the deuterated solvent mentioned; chemical shifts are expressed in parts per million as a δ value relative to the shift of the tetramethylsilane used as a reference. LC/MS was performed on a Waters HPLC with a 2996 photodiode array detector coupled to an LCT TOF mass spectrometer with electrospray ionization. The HPLC method was as follows: column used, Waters Xterra RP18 (3.5 μm, 50 × 2.1 mm i.d.); solvents, (A) water + 0.01% formic acid and (B) CH_3CN + 0.01% formic acid; gradient method, from 95/5 A/B at time 0 to 100% B after 4 min and then 100% B for 3 min. The purity of the described compounds was >98% according to HPLC analysis. Optical rotations ($[\alpha]_D^{23}$ were recorded on a Propol polarimeter. Specific rotations are given as degrees per decimeter, and the concentrations c are reported as grams per 100 mL of the specific solvent and were recorded at 23 °C.

Preparation of (±)-11b. *Methyl 2-(4-Acetoxyphenyl)-2-bromopropionate (**7**). Step 1: Methyl 2-(4-Hydroxyphenyl)propionate.* Thionyl chloride (25 mL, 0.35 mol) was added dropwise for 15 min at 0 °C to a solution of 2-(4-hydroxyphenyl)propanoic acid (**6**; 25 g, 0.15 mol) in methanol (500 mL); an exothermic reaction occurred. After 3.5 h at 0 °C, the mixture was concentrated and quenched with water, extracted with ethyl acetate, washed with water, and dried over $MgSO_4$. After concentration, methyl 2-(4-hydroxyphenyl)propionate was obtained as a brown oil (34.7 g, >100%) and used directly for the next step. ^{1}H NMR (400 MHz, $CDCl_3$): δ 1.48 (d, J = 7.2 Hz, 3H), 3.67 (m, 4H), 6.78 (d, J = 8.5 Hz, 2H), 7.17 (d, J = 8.5 Hz, 2H).

Step 2: Methyl 2-(4-Acetoxyphenyl)propionate. K_2CO_3 (31.05 g, 0.22 mol) was added at rt to a solution of the product obtained in step 1 (34.7 g) in THF (450 mL). Acetic anhydride (21 mL, 0.22 mol) was added dropwise for 10 min at 0 °C, giving rise to an exothermic reaction. After one night at rt, the mixture was filtered and rinsed with THF, and the filtrate was concentrated to provide methyl 2-(4-acetoxyphenyl)propionate as a colorless oil (42.3 g, >100%), used as such for the next step. ^{1}H NMR (400 MHz, $CDCl_3$): δ 1.50 (d, J = 7.2 Hz, 3H), 2.30 (s, 3H), 3.67 (s, 3H), 3.73 (q, J = 7.2 Hz, 1H), 7.05 (d, J = 8.4 Hz, 2H), 7.31 (d, J = 8.4 Hz, 2H). LC/MS: m/z 223 $[M + H]^+$, 240 $[M + H_2O]^+$, 264 $[M + CH_3CN]^+$.

Step 3: Methyl 2-(4-Acetoxyphenyl)-2-bromopropionate. *N*-Bromosuccinimide (32.04 g, 0.18 mol) and AIBN (2.95 g, 0.018 mol) were added to a solution of the compound obtained in step 2 (42.3 g) in carbon tetrachloride (500 mL). After 7 h under reflux, another batch of *N*-bromosuccinimide (13.35 g, 75 mmol) and AIBN (1.23 g, 7.5 mmol) were added, and reflux was maintained overnight. The mixture was then filtered, the solid was washed with dichloromethane, and the filtrate was concentrated. The residue was purified by chromatography (eluting with dichloromethane) to yield the title compound as an oil (48 g, 100%). ^{1}H NMR (400 MHz, $CDCl_3$): δ 2.30 (s, 6H), 3.79 (s, 3H), 7.09 (d, J = 8.8 Hz, 2H), 7.59 (d, J = 8.9 Hz, 2H). LC/MS: m/z 179 $[M + H - Br - MeCO]^+$.

*Methyl 2-(4-Hydroxyphenyl)-2-(methylamino)propionate (**8**).* A saturated solution of methylamine in ethanol (40 mL) was added at rt to bromo ester **7** (8.12 g, 27 mmol) dissolved in THF (160 mL). The mixture became pale yellow with formation of an insoluble substance. After 30 min at rt, the mixture was filtered and concentrated. The residue (yellow oil, 9.1 g) was purified by chromatography (eluting with 95/5 dichloromethane/methanol) to yield a pale yellow oil which was crystallized in isopropyl ether. After filtration and drying, the title compound was obtained (2.46 g, 43%) as a white powder. After evaporation, the filtrate provided a second crop of amorphous **8** (2 g, 35%) as a pale yellow oil. ^{1}H NMR (400 MHz, $CDCl_3$): δ 1.65 (s, 3H), 2.30 (s, 3H), 3.72 (s, 3H), 6.76 (d, J = 8.8 Hz, 2H), 7.29 (d, J = 8.8 Hz, 2H). LC/MS: m/z 179 $[M - MeNH]^+$.

*4-Cyano-3-(trifluoromethyl)phenyl Isocyanate (**10b**).* Triphosgene (21.16 g, 71.3 mmol) was dissolved in toluene (100 mL). A solution of aniline **9b** (20 g, 0.107 mol) in dioxane (125 mL) was added dropwise at rt over 1.5 h. The mixture was heated to 110 °C, a pronounced release of gas took place, and then an insoluble brown substance appeared. After 2 h under reflux, stirring was maintained at rt overnight. The insoluble matter was filtered off and washed with toluene. The filtrate was concentrated under vacuum to provide the title compound (21.8 g, 96%). It was stored at 4 °C as a 2 M solution in THF to be used quickly without purification for the next step.

*4-[3,4-Dimethyl-2,5-dioxo-4-(4-hydroxyphenyl)imidazolidin-1-yl]-2-(trifluoromethyl)benzonitrile ((±)-**11b**).* A 2 M solution of isocyanate **10b** in THF (940 μL, 1.88 mmol) was introduced in four portions to amino ester **8** (196 mg, 0.94 mmol) dissolved in THF (4 mL) over 5 h at rt. The mixture was then heated to reflux for 1 h. The insoluble matter was filtered and rinsed with THF, and the filtrate was evaporated. The residue was purified by chromatography while eluting with 30−40% ethyl acetate in heptane to provide the title compound (350 mg, 96%) as a white solid. Mp = 136 °C. ^{1}H NMR (400 MHz, $CDCl_3$): δ 1.96 (s, 3H), 2.97 (s, 3H), 6.92 (d, J = 8.8 Hz, 2H), 7.24 (d, J = 8.8 Hz, 2H), 7.94 (d, J = 8.4 Hz, 1H), 8.02 (dd, J = 1.8 and 8.5 Hz, 1H), 8.17 (d, J = 1.6 Hz, 1H). LC/MS: m/z 388 $[M - H]^-$, 777 $[2M - H]^-$.

*1-(3,4-Dichlorophenyl)-3,4-dimethyl-4-(4-hydroxyphenyl)-2-thioxoimidazolidin-5-one ((±)-**13a**).* Using isothiocyanate **12a** (Aldrich) and the amino ester **8** (0.48 g, 2.3 mmol), the procedure described above to prepare (±)-**11b** gave rise to the title compound (0.69 g, 77%). Mp = 194 °C. ^{1}H NMR (400 MHz, $CDCl_3$): δ 1.97 (s, 3H), 3.23 (s, 3H), 6.87 (d, J = 8.3 Hz, 2H), 7.15 (d, J = 8.3 Hz, 2H), 7.25 (m, 1H), 7.50 (m, 1H), 7.58 (m, 1H). LC/MS: m/z 379/381 $[M - H]^-$.

Preparation of (+)-11b and (−)-11b: Resolution of (±)-11b by Chiral HPLC. The racemic (±)-**11b** was resolved at 25 °C by chiral HPLC over a column of Chiralpak AD, 10 μm (250 × 4.6 mm i.d.). Elution was performed with a mixture of heptane/ethanol/methanol (80/10/10) (flow rate 1 mL/min, detection UV 220 nm). Following six consecutive injections and recycling of the unresolved fraction, 1.39 g of racemate provided 595 mg of (−)-**11b** eluted first (retention time 10.8 min) and 501 mg of (+)-**11b** eluted second (retention time 13.9 min).

Synthesis of (*R*)-(+)-11b. *(*R*)-4-[2,5-Dioxo-4-(4-methoxyphenyl)-4-methylimidazolidin-1-yl]-2-(trifluoromethyl)benzonitrile ((*R*)-(+)-**21b**).* A 2 M solution of isocyanate **10b** (9.5 mL, 19 mmol) in THF was added to a solution of the amino ester (*R*)-(−)-**20** (3.1 g, 14.8 mmol) in THF (60 mL) under an argon atmosphere. After 20 min at rt, triethylamine (2 mL, 14.8 mmol) was added, and the mixture was heated under reflux for 2 h. After cooling, the mixture was evaporated to dryness, and the residue was purified by chromatography, eluting with heptane/ethyl acetate (2/1). The title compound was obtained as a white resin (5.5 g, 95%). $[\alpha]_D^{23}$ = +26.4 (c 1, MeOH). ^{1}H NMR (400 MHz, $CDCl_3$): δ 1.97 (s, 3H), 3.84 (s, 3H), 6.22 (s, 1H), 6.97 (d, J = 8.9 Hz, 2H), 7.47 (d, J = 8.9 Hz, 2H), 7.92 (d, J = 8.4 Hz, 1H), 7.98 (dd, J = 2 and 8.4 Hz, 1H), 8.12 (d, J = 1.6 Hz, 1H). LC/MS: m/z 388 $[M - H]^-$, 390 $[M + H]^+$.

*(R)-4-[3,4-Dimethyl-2,5-dioxo-4-(4-hydroxyphenyl)imidazolidin-1-yl]-2-(trifluoromethyl)benzonitrile ((R)-(+)-**11b**). Step 1: (R)-4-[3,4-Dimethyl-2,5-dioxo-4-(4-methoxyphenyl)imidazolidin-1-yl]-2-(trifluoromethyl)benzonitrile.* To a solution of (*R*)-(+)-**21b** (5.4 g, 13.87 mmol) in DMF (100 mL) under argon was added a suspension of sodium hydride, 55% in oil (908 mg, 20.8 mmol), batchwise at 0 °C.

dx.doi.org/10.1021/jm300249m | J. Med. Chem. 2012, 55, 8225−8235

The mixture was stirred at 0 °C for 15 min, then methyl iodide (1.75 mL, 28 mmol) was added, and the mixture was stirred at rt for a further 2 h. The mixture was poured into iced water, and the product was extracted with ethyl acetate. The organic phases were washed with a saturated aqueous $NaHCO_3$ solution and then with brine. After drying over $MgSO_4$, filtration, and concentration, the residue was purified by chromatography, eluting with a 2/1 heptane/ethyl acetate mixture. The title compound (4.5 g, 80%) was obtained in the form of a white solid. $[\alpha]_D^{23}$ = +28.2 (*c* 1, MeOH). ^{1}H NMR (400 MHz, $CDCl_3$): δ 1.95 (s, 3H), 2.95 (s, 3H), 3.85 (s, 3H), 6.98 (d, *J* = 8.9 Hz, 2H), 7.28 (d, *J* = 8.9 Hz, 2H), 7.91 (d, *J* = 8.5 Hz, 1H), 8.02 (dd, *J* = 2 and 8.5 Hz, 1H), 8.18 (d, *J* = 1.8 Hz, 1H). LC/MS: *m*/*z* 404 $[M + H]^+$.

*Step 2: (R)-4-[3,4-Dimethyl-2,5-dioxo-4-(4-hydroxyphenyl)-imidazolidin-1-yl]-2-(trifluoromethyl)benzonitrile ((R)-(+)-**11b**).* Boron trifluoride−dimethyl sulfide complex (7.83 mL, 744 mmol) was added dropwise to a solution of the product of step 1 (3 g, 7.44 mmol) in dichloromethane (70 mL). After 24 h at rt, a saturated aqueous $NaHCO_3$ solution was added until pH 8, and then the product was extracted with dichloromethane. The organic phase was washed with brine and dried over $MgSO_4$. After filtration and concentration to dryness, the residue was purified by chromatography, eluting with a 2/1 heptane/ethyl acetate mixture. The title compound was obtained in the form of a white solid (2.8 g, 96%). Mp = 150.7 °C. $[\alpha]_D^{23}$ = +29.2 (*c* 1, MeOH). ^{1}H NMR (400 MHz, $CDCl_3$): δ 1.96 (s, 3H), 2.97 (s, 3H), 6.93 (d, *J* = 8.6 Hz, 2H), 7.24 (d, *J* = 8.6 Hz, 2H), 7.94 (d, *J* = 8.4 Hz, 1H), 8.02 (dd, *J* = 2 and 8.5 Hz, 1H), 8.18 (d, *J* = 1.5 Hz, 1H). LC/MS: *m*/*z* 388 $[M - H]^-$.

Synthesis of (*S*)-(−)-11b. *(S)-4-[2,5-Dioxo-4-(4-methoxyphenyl)-4-methylimidazolidin-1-yl]-2-(trifluoromethyl)benzonitrile ((S)-(−)-**21b**).* Starting from the amino ester (*S*)-(+)-**20** (540 mg, 2.58 mmol) and the isocyanate **10b** according to the protocol described above to prepare (*R*)-(+)-**21b**, the title compound was obtained in the form of a white solid (965 mg, 96%). $[\alpha]_D^{23}$ = −26.4 (*c* 1, MeOH). ^{1}H NMR (400 MHz, $CDCl_3$): δ 1.95 (s, 3H), 3.85 (s, 3H), 6.98 (d, *J* = 8.9 Hz, 2H), 7.27 (d, *J* = 8.9 Hz, 2H), 7.91 (d, *J* = 8.5 Hz, 1H), 8.02 (dd, *J* = 2 and 8.5 Hz, 1H), 8.17 (s, 1H). LC/MS: *m*/*z* 388 $[M - H]^-$, 431 $[M + H + CH_3CN]^+$.

*(S)-4-[3,4-Dimethyl-2,5-dioxo-4-(4-hydroxyphenyl)imidazolidin-1-yl]-2-(trifluoromethyl)benzonitrile ((S)-(−)-**11b**). Step 1: (S)-4-[3,4-Dimethyl-2,5-dioxo-4-(4-methoxyphenyl)imidazolidin-1-yl]-2-(trifluoromethyl)benzonitrile.* (*S*)-(−)-**21b** (915 mg, 2.35 mmol) was treated according to the protocol described above to prepare (*R*)-(+)-**11b** (MeI, NaH, DMF) to provide the title compound (1.15 g, >100%).

*Step 2: (S)-4-[3,4-Dimethyl-2,5-dioxo-4-(4-hydroxyphenyl)-imidazolidin-1-yl]-2-(trifluoromethyl)benzonitrile ((S)-(−)-**11b**).* The compound obtained above (1.15 g) was treated following the procedure used to prepare (*R*)-(+)-**11b** (BF_3.Me_2S, CH_2Cl_2). The title compound was obtained as a white solid (867 mg, 95%). Mp = 150.5 °C. $[\alpha]_D^{23}$ = −28 (*c* 1, MeOH). ^{1}H NMR (400 MHz, $CDCl_3$): δ 1.96 (s, 3H), 2.97 (s, 3H), 6.92 (d, *J* = 8.4 Hz, 2H), 7.24 (d, *J* = 8.8 Hz, 2H), 7.93 (d, *J* = 8.6 Hz, 1H), 8.02 (dd, *J* = 1.1 and 8.6 Hz, 1H), 8.18 (br s, 1H).

Synthesis of (*R*)-(+)-13a. *(R)-1-(3,4-Dichlorophenyl)-3,4-dimethyl-4-(4-methoxyphenyl)-2-thioxoimidazolidin-5-one (**24a**).* Triethylamine (0.185 mL, 1.33 mmol) and isothiocyanate **12a** (Aldrich, 0.230 g, 1.13 mmol) were added to a solution of **23** (0.246 g, 1.10 mmol) in THF (10 mL). The mixture was stirred at rt for 1 h and then evaporated to dryness. The residue was diluted with water, extracted with ethyl acetate, dried over $MgSO_4$, filtered, and evaporated. The crude product was purified by chromatography, eluting with 20% ethyl acetate in heptane. The title compound was obtained as a white solid (0.41 g, 95%). ^{1}H NMR (400 MHz, $CDCl_3$): δ 1.96 (s, 3H), 3.22 (s, 3H), 3.84 (s, 3H), 6.99 (d, *J* = 7.8 Hz, 2H), 7.20 to 7.27 (m, 3H), 7.49 (d, *J* = 2.4 Hz, 1H), 7.57 (d, *J* = 8.6 Hz, 1 H). LC/MS: *m*/*z* 395/397 $[M + H]^+$.

*(R)-1-(3,4-Dichlorophenyl)-3,4-dimethyl-4-(4-hydroxyphenyl)-2-thioxoimidazolidin-5-one ((R)-(+)-**13a**).* Boron trifluoride−dimethyl sulfide complex (1 mL, 9.5 mmol) was added to a solution of **24a** (0.4 g, 1.01 mmol) in dichloromethane (30 mL). The mixture was stirred at rt for 24 h, then poured into a saturated aqueous $NaHCO_3$ solution, and extracted with ethyl acetate. The organic layer was dried over $MgSO_4$, filtered, and evaporated. The residue was purified by crystallization in a mixture of dichloromethane/methanol/ether/pentane and then crystallized again in dichloromethane. The title compound was obtained as white crystals (0.27 g, 70%). Mp = 192 °C. $[\alpha]_D^{23}$ = +39.6 (c 1.05, MeOH). ^{1}H NMR (400 MHz, $CDCl_3$): δ 1.96 (s, 3H), 3.24 (s, 3H), 6.90 (d, *J* = 8.8 Hz, 2H), 7.17 (d, *J* = 8.8 Hz, 2H), 7.25 (dd, *J* = 2.4 and 8.6 Hz, 1H), 7.50 (d, *J* = 2.3 Hz, 1H), 7.58 (d, *J* = 8.6 Hz, 1H). LC/MS: *m*/*z* 379/381 $[M - H]^-$, 381/383 $[M + H]^+$.

In Vitro Transactivation Assay. The in vitro molecular efficacy and potency were assessed using a stable cell line derived from Hela cells expressing hAR and a reporter gene placed under the transcriptional control of the probasin AREs. This transactivation assay allows the identification of pure agonists (such as testosterone and DHT), partial agonists, and antagonists.

In the Monod−Wyman−Changeux model,[14] the receptor is constantly in interconversion equilibrium between two states (active A and inactive R), and any ligand of the receptor actually has two molecular affinities for the receptor: one for the active state A (denoted K_A) and one for the inactive state R (denoted K_R). The ratio of the affinities of the compound for the two states (K_R/K_A) is called the molecular efficacy of the compound. The position of the equilibrium in the absence of ligand is defined by the ratio [R]/[A] and is equal to a constant classically denoted L_0, $L_{[X]}$ being the value of this ratio in the presence of the ligand at concentration [X]. Applying the law of mass action to each of the states, $[RX] = [R][X]/K_R$ and $[AX] = [A][X]/K_A$, leads to the key expression $L_{[X]} = L_0(1 + [X]/K_R)/(1 + [X]/K_A)$. At saturating concentrations of the ligand a limit value is obtained: $L_\infty = L_0(K_A/K_R)$. This is precisely the equation separating, in the expression of molecular efficacy, the contribution of the tissue from that of the compound: the ratio of the affinities of the compound for the two states (K_R/K_A, i.e., the way the compound does or does not discriminate between the two states) is called the molecular efficacy of the compound and determines its maximal effect on the equilibrium of active and inactive receptor states, whereas L_0 determines the contribution of the tissue. Efficacies reported in the paper are the ratio K_R/K_A related to the compound contribution. Applying the law of mass action to each of the two states also leads to the potency equation: $1/K_d = L_0/(1 + L_0)(1/K_R) + 1/(1 + L_0)(1/K_A)$, expressing that the apparent affinity is simply the harmonic mean of the two molecular affinities, weighted by the initial position of the equilibrium.

We therefore used a Schild-type curve-shift paradigm approach by crossing a range of concentrations of our compound and a range of concentrations of DHT as the reference agonist.[23] We analyzed both the rightward shift of the DHT curve induced by the antagonist activity of our compound and the upward shift of its lower plateau induced by the agonist activity of our compound. To reach the two molecular affinities K_A and K_R of our SARM compounds, we built the mathematical theoretical behavior of our system with parametrized equations where K_A and K_R are the parameters identified by fitting the bundle of curves from the curve-shift paradigm as a whole. From these two identified parameters, potency and molecular efficacy were calculated as indicated.

In Vivo Pharmacology. All procedures were performed in accordance with national and European legislations on animal experimentation.

The dissociated activity of the compounds was tested in an adapted model of castrated immature young rats which is widely recognized for evaluating the anabolic and androgenic effects of androgens on muscles and on genitalia.[16b] Castrated rats were left untreated for one week and then treated for four days with test compound. Castration resulted in a rapid atrophy of the VP as well as of the anus-lifting muscle LA. These effects are completely compensated by an exogenous administration of androgens. The stringency of therapeutic setting is greater than that of prophylactic setting and allows detection of more potent myotrophic/anabolic compounds. After four days of treatment, the activity of the compound was expressed as a percentage

and calculated using the following formula: (W/BW treated − W/BW ORX)/(W/BW sham − W/BW ORX) × 100, where W is weight and BW is body weight. The dissociated activity of the test compound was expressed as the ratio between the dose displaying 50% activity (A_{50}) on VP and LA.

The bone activity of the compounds was tested using rats castrated at six months of age and treated for three months, immediately after castration, either with test compound or with vehicle (EtOH/corn oil, 10/90). Sham-operated animals received vehicle treatment. Densitometric analysis was performed on tibias using the Stratec pQCT XCT Research SA+ (version 5.4B; Norland Medical Systems, White Plains, NY) at 70 μm resolution. The trabecular volumetric BMD was measured by metaphyseal pQCT scans positioned 1 mm from the distal growth plate and corresponding to 6% of the total length of the tibia. Micro computed tomography (μCT) scans of the metaphyseal region of the tibias were performed at an isotropic resolution of 9 μm to obtain the trabecular bone structural parameter (BV/TV) using the Scanco Medical μCT scanner CT (μCT 20; Scanco Medical AG, Bassersdorf, Switzerland). The mean tissue of the scanned area was between 1.0 and 3.0 mm from the growth plate in the trabecular bone of the tibial proximal metaphysis.

After removal of the fibula, a proximal tibia compression test was performed using axial compression of the tibia plateau, the shaft being fixed in methyl methacrylate cement (Technovit 4071, Heraeus Kulzer GmbH, Wehrheim, Germany). A three-point bending test of the femur was also performed. The femur was placed in the material testing machine on two supports separated by a distance of 20 mm, and load was applied on the middle of the shaft. The mechanical resistance to failure was tested using a servo-controlled electromechanical system (Instron 1114, Instron Corp., High Wycombe, U.K.) with the actuator displaced at 2 mm/min. Both displacement and load were recorded. The ultimate strength (maximal load, N) was calculated.

Structure Determination of hAR LBD Complexes with (+)-11b and (+)-13a. Expression, purification, and crystallization have been reported previously.[17] More details are available in the Supporting Information. Briefly, the structures were solved by the molecular replacement method using the model of hAR LBD complexed to DHT (PDB code 2AMA) as a search model.[18] Refinement was conducted with SHELXL,[24] and rebuilding was done with Coot.[25] The final model for the complex with (+)-**11b** has an R factor of 0.192 (R_{free} = 0.230) and contains 2339 atoms (2006 protein atoms, 215 water molecules, 90 undecapeptide atoms, and the 28 atoms of (+)-**11b**). The final model for the complex with (+)-**13a** has an R factor of 0.173 (R_{free} = 0.211) and contains 2388 atoms (2024 protein atoms, 250 water molecules, 90 undecapeptide atoms, and the 24 atoms of (+)-**13a**). The coordinates have been deposited in the PDB with accession codes 3V49 and 3V4A.

■ ASSOCIATED CONTENT

Ⓢ Supporting Information

Preparation and characterization data for intermediates and final compounds (±)-**10c−f**, (±)-**11a,c−f**, **12b**, (±)-**13b**, **14**, (±)-**15b**, **16**, (±)-**17b**, (−)-**19**, (+)-**20**, (−)-**20**, (+)-**21c**, (+)-**11c**, **22**, and (−)-**23** along with an X-ray data processing and refinement statistics table. This material is available free of charge via the Internet at http://pubs.acs.org.

Accession Codes

PDB codes: (+)-**11b**, 3V49; (+)-**13a**, 3V4A.

■ AUTHOR INFORMATION

Corresponding Author

*Phone: +33 149424687. Fax: +33 149424658. E-mail: pierre.deprez@glpg.com.

Present Addresses

[§]Directorate Organic Chemistry, European Patent Office, Patentlaan 2, 2288 EE Rijswijk, The Netherlands.

[∥]Isochem, 4 avenue Philippe Lebon, 92230 Gennevilliers, France.

[⊥]Institut de Recherche Servier, 125 chemin de ronde, 78290 Croissy-sur-Seine, France.

Notes

The authors declare no competing financial interest.

■ ACKNOWLEDGMENTS

We thank Gaëtan Gitton and Karen Séchet for their excellent technical assistance during the syntheses. We also thank Kara Bortone for her careful review of the manuscript. The chiral chromatographic separations were efficiently performed by Serge Droux and his team (Kyralia SAS, Parc Biocitech, Romainville, France). Philippe Bénas is thanked for assistance during crystallographic data collection. The biomechanical experiments on bone were efficiently realized by Patrick Ammann and his team (Fondation Recherches Médicales, Geneva, Switzerland).

■ ABBREVIATIONS USED

SARM, selective androgen receptor modulator; AR, androgen receptor; ORX, orchidectomized; T, testosterone; TP, testosterone propionate; DHT, 5α-dihydrotestosterone; SERMs, nonsteroidal selective estrogen receptor modulators; SAR, structure−activity relationship; AR LBD, ligand-binding domain of the androgen receptor; ARE, androgen-responsive element; LA, levator ani muscle; VP, ventral prostate; BMD, bone mineral density; HDL, high-density lipoprotein

■ REFERENCES

(1) Kaufman, J. M.; Vermeulen, A. The Decline in Androgen Levels in Elderly Men and Its Clinical and Therapeutic Implications. *Endocr. Rev.* **2005**, *26*, 833−876.

(2) Rosario, E. R.; Pike, C. J. Androgen Regulation of β-Amyloid Protein and the Risk of Alzheimer's Disease. *Brain Res. Rev.* **2008**, *57*, 444−453.

(3) (a) Snyder, P. J.; Peachey, H.; Hannoush, P.; Berlin, J. A.; Loh, L.; Lenrow, D. A.; Holmes, J. H.; Dlewati, A.; Santanna, J.; Rosen, C. J.; Strom, B. L. Effect of Testosterone Treatment on Body Composition and Muscle Strength in Men over 65 of Age. *J. Clin. Endocrinol. Metab.* **1999**, *84*, 2647−2653. (b) Bhasin, S.; Woodhouse, L.; Casaburi, R.; Singh, A. B.; Mac, R. P.; Lee, M.; Yarasheski, K. E.; Sinha-Hikim, I.; Dzekov, C.; Dzekov, J.; Magliano, L.; Storer, T. W. Older Men Are as Responsive as Young Men to the Anabolic Effects of Graded Doses of Testosterone on Skeletal Muscle. *J. Clin. Endocrinol. Metab.* **2005**, *90*, 678−688.

(4) (a) Liu, P. Y.; Swerdloff, R. S.; Veldhuis, J. D. The Rational, Efficacy and Safety of Androgen Therapy in Older Men: Future Research and Current Practice Recommendations. *J. Clin. Endocrinol. Metab.* **2004**, *89*, 4789−4796. (b) Rhoden, E. L.; Morgentaler, A. Risks of Testosterone-Replacement Therapy and Recommendations. *N. Engl. J. Med.* **2004**, *350*, 482−492.

(5) (a) Dalton, J. T.; Mukherjee, A.; Zhu, Z.; Kirkovsky, L.; Miller, D. D. Discovery of Nonsteroidal Androgens. *Biochem. Biophys. Res. Commun.* **1998**, *244*, 1−4. (b) Hamann, L. G.; Mani, N. S.; Davis, R. L.; Wang, X. N.; Marschke, K. B.; Jones, T. K. Discovery of a Potent, Orally Active, Nonsteroidal Androgen Receptor Agonist: 4-Ethyl-1,2,3,4-tetrahydro-6-(trifluoromethyl)-8-pyridono[5,6-*g*]quinoline (LG121071). *J. Med. Chem.* **1999**, *42*, 210−212.

(6) (a) Sato, M.; Grese, T. A.; Dodge, J. A.; Bryant, H. U.; Turner, C. H. Emerging Therapies for the Treatment of Postmenopausal Osteoporosis. *J. Med. Chem.* **1999**, *42*, 1−24. (b) Delmas, P. D.; Ensrud, K. E.; Adachi, J. D.; et al. Efficacy of Raloxifene on Vertebral Fracture Risk Reduction in Postmenopausal Women with Osteoporosis: Four-Year Results from a Randomized Clinical Trial. *J. Clin.*

Endocrinol. Metab. **2002**, *87*, 3609−3617. (c) Jordan, V. C. Antiestrogens and Selective Estrogen Receptor Modulators as Multifunctional Medicines. 1. Receptor Interactions. *J. Med. Chem.* **2003**, *46* (6), 883−908. (d) Jordan, V. C. Antiestrogens and Selective Estrogen Receptor Modulators as Multifunctional Medicines. 2. Clinical Considerations and New Agents. *J. Med. Chem.* **2003**, *46* (7), 1081−1111.

(7) (a) Cadilla, R.; Turnbull, P. Selective Androgen Receptor Modulators in Drug Discovery: Medicinal Chemistry and Therapeutic Potential. *Curr. Top. Med. Chem.* **2006**, *6*, 245−270. (b) Kilbourne, E. J.; Moore, W. J.; Freedman, L. P.; Nagpal, S. Selective Androgen Receptor Modulators for Frailty and Osteoporosis. *Curr. Opin. Invest. Drugs* **2007**, *8*, 821−829. (c) Gao, W.; Dalton, J. T. Expanding the Therapeutic Use of Androgens via Selective Androgen Receptor Modulators (SARMs). *Drug Discovery Today* **2007**, *12*, 241−248. For a review, see: Mohler, M. L.; Bohl, C. E.; Jones, A.; Coss, C. C.; Narayanan, R.; He, Y; Hwang, D. J.; Dalton, J. T.; Miller, D. D. Nonsteroidal Selective Androgen Receptor Modulators (SARMs): Dissociating the Anabolic and Androgenic Activities of the Androgen Receptor for Therapeutic Benefit. *J. Med. Chem.* **2009**, *52* (12), 3598−3617.

(8) (a) Yin, D.; Gao, W.; Kearbey, J. D.; Xu, H.; Chung, K.; He, Y.; Marhefka, C. A.; Veverka, K. A.; Miller, D. D.; Dalton, J. T. Pharmacodynamics of Selective Androgen Receptor Modulators. *J. Pharmacol. Exp. Ther.* **2003**, *304* (3), 1334−1340. (b) Marhefka, C. A.; Gao, W.; Chung, K.; Kim, J.; He, Y.; Yin, D.; Bohl, C.; Dalton, J. T.; Miller, D. D. Design, Synthesis, and Biological Characterization of Metabolically Stable Selective Androgen Receptor Modulators. *J. Med. Chem.* **2004**, *47* (4), 993−998.

(9) Kim, J.; Wu, D.; Hwang, D. J.; Miller, D. D.; Dalton, J. T. The *para* Substituent of *S*-3-(Phenoxy)-2-hydroxy-2-methyl-*N*-(4-nitro-3-trifluoromethyl-phenyl)-propionamides Is a Major Structural Determinant of in Vivo Disposition and Activity of Selective Androgen Rreceptor Modulators. *J. Pharmacol. Exp. Ther.* **2005**, *315* (1), 230−239.

(10) Ostowski, J.; Kuhns, J. E.; Lupisella, J. A.; Manfredi, M. C.; Beehler, B. C.; Krystek, S. R., Jr.; Bi, Y.; Sun, C.; Seethala, R.; Golla, R.; Sleph, P. G.; Fura, A.; An, Y.; Kish, K. F.; Sack, J. S.; Mookhtiar, K. A.; Grover, G. J.; Hamann, L. G. Pharmacological and X-ray Structural Characterization of a Novel Selective Androgen Receptor Modulator: Potent Hyperanabolic Stimulation of Skeletal Muscle with Hypostimulation of Prostate in Rats. *Endocrinology* **2007**, *148* (1), 4−12.

(11) Narayanan, R.; Mohler, M. L.; Bohl, C. E.; Miller, D. D.; Dalton, J. T. Selective Androgen Receptor Modulators in Preclinical and Clinical Development. *Nucl. Recept. Signaling* **2008**, *6* (1), e010.

(12) (a) Raynaud, J. P.; Bonne, C.; Moguilewsky, M.; Lefebvre, F. A.; Belanger, A.; Labrie, F. The Pure Antiandrogen RU23908 (Anandron), a Candidate of Choice for the Combined Antihormonal Treatment of Prostate Cancer: A Review. *Prostate* **1984**, *5* (3), 299−311. (b) Harris, M. G.; Coleman, S. G.; Faulds, D.; Chrisp, P. Nilutamide. A Review of Its Pharmacodynamic and Pharmacokinetic Properties, and Therapeutic Efficacy in Prostate Cancer. *Drugs Aging* **1993**, *3* (1), 9−25.

(13) (a) Cheng, P. T. W. U.S. Patent 5,770,615. (b) Washburn, W. N.; et al. BMS-201620: A Selective Beta 3 Agonist. *Bioorg. Med. Chem. Lett.* **2004**, *14*, 3525−3529.

(14) Garcia, H. G.; Kondev, J.; Orme, N.; Theriot, J. A.; Phillips, R. Thermodynamics of Biological Processes. *Methods Enzymol.* **2011**, *492*, 27−59.

(15) (a) Battmann, T.; Bonfils, A.; Branche, C.; Humbert, J.; Goubet, F.; Teutsch, G.; Philibert, D. RU58841, a New Specific Topical Antiandrogen: A Candidate of Choice for the Treatment of Acne, Androgenetic Alopecia and Hirsutism. *J. Steroid Biochem. Mol. Biol.* **1994**, *48* (1), 55−60. (b) Van Dort, M. E.; Jung, Y. W. Synthesis and Structure-Activity Studies of Side-Chain Derivatized Arylhydantoins for Investigation as Androgen Receptor Radioligands. *Bioorg. Med. Chem. Lett.* **2001**, *11* (8), 1045−1047.

(16) (a) Eisenberg, E.; Gordan, G. S. The Levator Ani of the Rat as an Index of Myotrophic Activity of Steroidal Hormones. *J. Pharmacol. Exp. Ther.* **1950**, *99* (1), 38−44. (b) Hershberger, L. G.; Shipley, E. G.; Meyer, R. K. Myotrophic Activity of 19-Nortestosterone and Other Steroids Determined by Modified Levator Ani Muscle Method. *Proc. Soc. Exp. Biol. Med.* **1953**, *83* (1), 175−180. (c) Kicman, A. T. Pharmacology of Anabolic Steroids. *Br. J. Pharmacol.* **2008**, *154* (3), 502−521.

(17) Thauvin, M.; Robin-Jagerschmidt, C.; Nique, F.; Mollat, P.; Fleury, D.; Prangé, T. Crystallization and Preliminary X-ray Analysis of the Human Androgen Receptor Ligand-Binding Domain with a Coactivator-Like Peptide and Selective Androgen Receptor Modulators. *Acta Crystallogr.* **2008**, *F64*, 1159−1162.

(18) Pereira de Jésus-Tran, K.; Cote, P. L.; Cantin, L.; Blanchet, J.; Labrie, F.; Breton, R. Comparison of Crystal Structures of Human Androgen Receptor Ligand-Binding Domain Complexed with Various Agonists Reveals Molecular Determinants Responsible for Binding Affinity. *Protein Sci.* **2006**, *15*, 987−999.

(19) Bourguet, W.; Germain, P.; Gronemeyer, H. Nuclear Receptor Ligand-binding Domains: Three-Dimensional Structures, Molecular Interactions and Pharmacological Implications. *Trends Pharmacol. Sci.* **2000**, *21*, 381−388.

(20) Bohl, C. E.; Wu, Z.; Chen, J.; Mohler, M. L.; Yang, J.; Hwang, D. J.; Mustafa, S.; Miller, D. D.; Bell, C. E.; Dalton, J. T. Effect of B-Ring Substitution Pattern on Binding Mode of Propionamide Selective Androgen Receptor Modulators. *Bioorg. Med. Chem. Lett.* **2008**, *18*, 5567−5570.

(21) Sack, J. S.; Kish, K. F.; Wang, C.; Attar, R. M.; Kiefer, S. E.; An, Y.; Wu, G. Y.; Scheffler, J. E.; Salvati, M. E.; Krystek, S. R., Jr.; Weinmann, R.; Einspahr, H. M. Crystallographic Structures of the Ligand-Binding Domains of the Androgen Receptor and Its T877A Mutant Complexed with the Natural Agonist Dihydrotestosterone. *Proc. Natl. Acad. Sci. U.S.A.* **2001**, *98* (9), 4904−4909.

(22) *Discovery Studio*, version 3.1; Accelrys Inc.: San Diego, CA, 2011.

(23) Arunklakshana, O.; Schild, H. O. Some Quantitative Uses of Drug Antagonists. *Br. J. Pharmacol. Chemother.* **1959**, *65*, 48−58.

(24) Sheldrick, G. M.; Schneider, T. R. SHELXL: High Resolution Refinement. *Methods Enzymol.* **1997**, *277*, 319−343.

(25) Emsley, P.; Cowtan, K. COOT: Model-Building Tools for Molecular Graphics. *Acta Crystallogr.* **2004**, *D60*, 2126−2132.